

THE BEAM TRACKING DURING THE FIRST FEW MILLISECONDS OF A LOW ENERGY BOOSTER *

Shinji Machida

University of Houston, Houston, Texas 77204
Texas Accelerator Center, The Woodlands, Texas 77381

Summary

The space charge effect in the presence of sextupole resonance was studied using the lattice of the SSC low energy booster. We performed the multiparticle tracking with a self-consistent charge distribution. When there are synchrotron oscillations, a slight emittance growth is observed, which differs from the result of non-self-consistent tracking. However, this growth cannot be caused by repeated crossing of resonances due to sextupole field in dipoles. The tracking result has shown that the emittance dilution of the whole beam should be considered instead of amplitude growth of some particular particles.

Introduction

The emittance degradation by space charge is inevitable in a proton synchrotron when the beam energy is low. This is a crucial problem in the design of high energy colliders such as the proposed SSC and high intensity proton accelerators ("Kaon Factory"). In the former, the emittance growth at low energy may result in the reduction of luminosity, while in the latter, the acceptable intensity is primarily limited by space charge.

Several studies have been done to investigate the space charge effect and emittance degradation. For instance, one of the theoretical studies explains the amplitude growth of a particle by the repeated crossing of a nonlinear resonance [1,2]. This happens when there is a large tune shift due to space charge which is modulated by a synchrotron oscillation, especially when the oscillating frequency is high, say, 0.01. Recent studies by tracking method have investigated the space charge effect numerically for particular machines, e.g., the SSC low energy booster [3] and the AGS booster [4].

The treatment of space charge in these studies, however, is not self-consistent or very limited in the number of particles when they try to take into account the change of beam distribution as a function of time. In the present study, we have used a supercomputer to estimate a beam shape evolution at each lattice element to make the treatment self-consistent with 1000 particles for 1024 turns in the SSC low energy booster. The only assumption made for the beam distribution is an elliptical symmetry in the physical horizontal-vertical plane. This is reasonable in the absence of strong coupling between two transverse directions.

Tracking Method

Evaluation of Space Charge

When an unbunched beam has uniform charge distribution in the transverse space with elliptic cross section, the space charge field can be calculated from the potential [5],

$$\phi(x, y) = -\lambda/(4\pi\epsilon_0) \times \begin{cases} \int_0^\infty \frac{x^2/(a^2+t)+y^2/(b^2+t)}{(a^2+t)^{1/2}(b^2+t)^{1/2}} dt, & \frac{x^2}{a^2} + \frac{y^2}{b^2} < 1, \\ \int_0^{t_0} \frac{1}{(a^2+t)^{1/2}(b^2+t)^{1/2}} dt + \int_{t_0}^\infty \frac{x^2/(a^2+t)+y^2/(b^2+t)}{(a^2+t)^{1/2}(b^2+t)^{1/2}} dt, & \frac{x^2}{a^2} + \frac{y^2}{b^2} > 1, \end{cases}$$

where $t_0(x, y)$ is the value of t_0 for which

$$x^2/(a^2 + t_0) + y^2/(b^2 + t_0) = 1,$$

with λ the charge per unit length. To obtain the electric field for an arbitrary distribution, we divided the beam into a number of disks, each with an uniform charge distribution as shown in Fig. 1. The electric field at an arbitrary point is the superposition of the electric fields due to each disk.

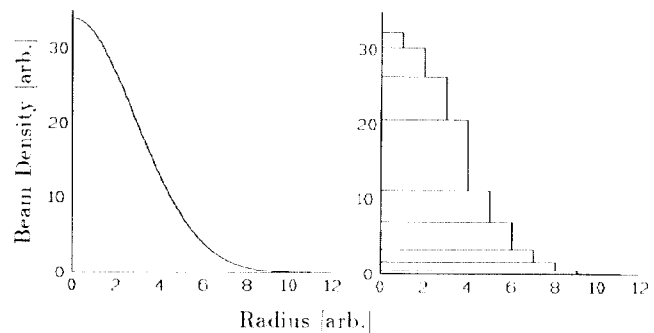


Fig. 1: Reconstruction of the beam distribution by using uniform disks. The height of each disk represents the density.

The optimum number of disks was determined taking into account a trade-off between the statistical fluctuation of the number of particles in each disk and roughness of the estimated field as a whole. If we took smaller number of disks, the number of particles in each disk should increase so that the accuracy of the field due to each disk would be better. However, the combined field would have a large error at a given position within the beam. The situation would be reversed if we took too many disks without increasing the total number of particles. Here we divided the beam into some 30 disks, since the field calculated from particles in these disks reproduced the analytical one most closely as shown in Fig. 2.

*Work supported by the U.S. Department of Energy under grant No. DE-FG05-87ER40374.

Modification in TEAPOT

We modified computer code TEAPOT [6] to have a capability to calculate the space charge effect as a kick. In this program, space charge kicks were introduced at the center of each quadrupole. With NEC SX-2 supercomputer, the typical CPU time with 1000 particles for 1024 turns in the SSC booster is approximately 25 minutes.

In order to check the program, we compared the tune shift (-0.11 for this case) obtained from tracking with the one based on the Laslett formula [7], when the initial distribution was K-V [8]. No difference was observed between these two within the expected error of FFT which was used to get tunes from 256 revolutions.

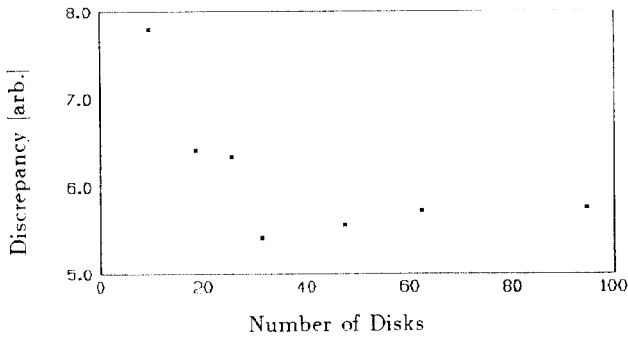


Fig. 2: Number of disks vs. integrated discrepancy between the field obtained from the tracking particles and the one of the analytical form for the Gaussian having a circular cross section.

Lattice, Magnet Imperfection and Beam Parameters

We used the SSC low energy booster for this study [3]. The lattice has sextupoles after each quadrupole to make the chromaticity zero. Although the momentum spread of the beam was not taken into account explicitly, these sextupoles for chromaticity correction were included in the tracking. There is no structure resonance of the third order near the working point because the superperiodicity is 2. The random sextupole in dipoles will be discussed below.

We simplified the linear elements in the machine by replacing each quadrupole by one thin lens kick, while the dipole was treated as a sector magnet. Furthermore, we simulated the random sextupole errors in all dipoles by introducing two pairs of normal sextupoles that drive resonances $3\nu_x = 35$ and $\nu_x + 2\nu_y = 35$.

The strength of these sextupoles were determined to produce the stopband width of 1.1×10^{-3} for both resonances. This is almost the same as the value estimated for the SSC booster [3] and for the Saturne II [9]. The stopbands are estimated from the expressions,

$$\Delta e = \frac{1}{8\pi B\rho} \epsilon_x^{1/2} \sum \beta_x^{3/2} B'' e^{i(3Q_x + 35\theta)},$$

$$(3\nu_x = 35),$$

$$\Delta e = \frac{1}{6\pi B\rho} \epsilon_x^{1/2} \left(1 + \frac{\epsilon_y}{4\epsilon_x}\right) \sum \beta_x^{1/2} \beta_y B'' e^{i(Q_x + 2Q_y + 35\theta)},$$

$$(\nu_x + 2\nu_y = 35),$$

where $Q_{x,y} = \int ds / \beta_{x,y} - \nu_{x,y} \theta$, $\beta_{x,y}$ are the betatron amplitude functions, B'' is the strength of each sextupole, $B\rho = 4.066$ T m, $\epsilon_{x,y} = 1.732 \times 10^{-6} \pi$ m rad. The widths of these stopbands were checked by a single particle tracking using the same lattice, which gave 1.1×10^{-3} and 1.2×10^{-3} respectively.

For an initial beam distribution, we took a Gaussian with the normalized rms emittance $\epsilon_{x,y} = 0.75 \times 10^{-6} \pi$ m rad but particles beyond 3σ are not used in the tracking.

Tracking Results

We observed the rms emittance, Twiss parameters $\beta_{x,y}$, $\alpha_{x,y}$, beam population as a function of the distance from the beam axis, and tune distribution of the beam after 1024 turns. The tune was found from the peak position of the Fourier power spectrum using the last 256 turns.

Figure 3 shows the beam population as a function of the distance from the beam axis and Fig. 4 shows tune distribution after 1024 turns. In both cases, there is no random sextupole or synchrotron oscillation. Different tune shifts for each particle give the tune spread a necktie shape. There is no significant change of the beam population after 1024 turns. Next we excited the sextupole pairs representing sextupole error field in dipoles. Some particles with a small amplitude should be close to the resonance line. From the result of the tracking we find no effect from the sextupoles.

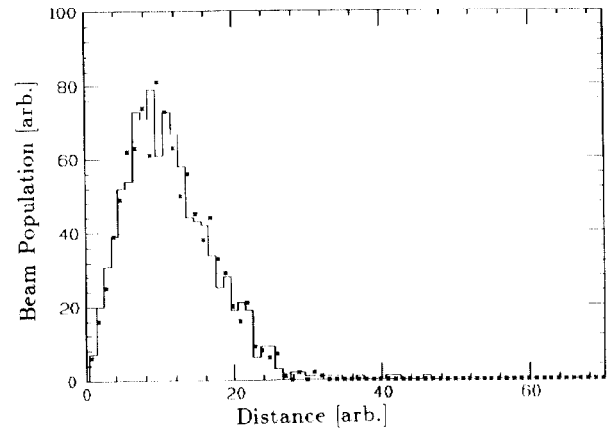


Fig. 3: Beam population as a function of the distance from the beam axis. The star mark indicates the population of the first turn and the histogram does the one after 1024 turns.

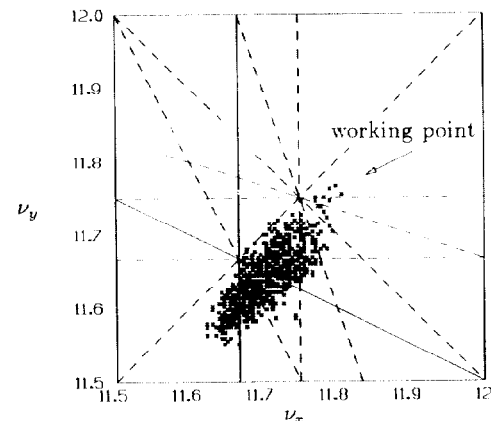


Fig. 4: Tune distribution after 1024 turns. Solid lines shows $3\nu_x = 35$ and $\nu_x + 2\nu_y = 35$ resonances.

When there is a synchrotron oscillation, the beam density varies along the bunch from a maximum at the center to zero at either end. Consequently, the tune shift of an individual particle oscillates at twice the synchrotron frequency,

$$\begin{aligned}\nu_{x,y} &= \nu_{0\ x,y} - \Delta \left[1 - \left(\frac{\phi_m}{\phi_{max}} \right)^2 \sin^2 \nu_s \theta \right] \\ &= \nu_{0\ x,y} - \Delta \left[1 - \frac{1}{2} \left(\frac{\phi_m}{\phi_{max}} \right)^2 + \frac{1}{2} \left(\frac{\phi_m}{\phi_{max}} \right)^2 \cos 2\nu_s \theta \right],\end{aligned}$$

where $\nu_{0\ x,y}$ is the tune without space charge, Δ is the maximum tune shift that depends on the transverse amplitude, ϕ_{max} is the bunch length, ϕ_m is the amplitude of synchrotron oscillation, and ν_s is the synchrotron tune. Repeated crossings of a resonance are generally considered to be a possible source of emittance growth.

To simulate this tune modulation and crossing, we varied the charge density of the beam such that the tune variation of the same time dependence as mentioned above would result. First the effect of the synchrotron oscillation alone was examined. Since all particles are assumed to have the same longitudinal amplitude, $(\phi_m/\phi_{max})^2 = 0.5$, the tune shift will oscillate between the maximum value and half of the maximum. This synchrotron oscillation makes the beam emittance in the y-direction grow about 30 %. Next we added the sextupole pairs representing sextupole error field in dipoles. The growth of the emittance is almost the same as the case without sextupole. In order to see the dependence on the sextupole strength, we increased the strength by an order of magnitude but no substantial change in the emittance growth was detected from this tracking.

Tables 1 and 2 summarize the rms emittance and Twiss parameters obtained in this study.

Table 1: The difference between the design lattice parameters and the Twiss parameters found from the tracking particles as an initial distribution.

	ϵ_x	β_x	α_x	ϵ_y	β_y	α_y
Design beam	.577 μ m	3.82m	0	.577 μ m	7.28m	0
Simulation	.571	3.72	-.0429	.578	7.20	-.0266

$\epsilon_{x,y}$ are unnormalized emittance.

Table 2: The rms emittance and Twiss parameters after 1024 turns for various conditions.

sxt	syn	ϵ_x	β_x	α_x	ϵ_y	β_y	α_y
-	-	.591 μ m (4%)	4.06m	-.0083	.635 μ m (10%)	7.61m	.0720
+	-	.567 (5%)	4.03	-.0202	.618 (7%)	7.42	.0737
-	+	.605 (6%)	3.90	.0220	.747 (29%)	7.61	-.0109
+	+	.607 (6%)	3.88	.0453	.722 (25%)	6.71	.0166
$\times 10$	+	.615 (8%)	3.93	-.0128	.720 (25%)	6.83	-.0490

where 'sxt' means the random sextupole and 'syn' stands for the synchrotron oscillation. The symbol '+' and '-' mean respectively with and without, and ' $\times 10$ ' indicates the increased sextupole strength.

If we abandon the self-consistent treatment and use the fixed charge distribution in calculating the space charge effect, we find somewhat different results. For example, with sextupole pairs and synchrotron oscillation, the rms emittance does not grow as much. See Table 3.

Table 3: The rms emittance and Twiss parameters after 1024 turns with non-self-consistent treatment.

sxt	syn	ϵ_x	β_x	α_x	ϵ_y	β_y	α_y
+	+	.579 (1%)	4.18	.0562	.617 (7%)	7.68	-.0387

Conclusion

Using the SSC low energy booster as a test case, we have investigated the space charge effect on the emittance dilution in the presence of sextupole resonances. The emphasis was placed on the self-consistent treatment of the changing charge distribution of the beam for which a large number of particles have been tracked. In addition, the multiple crossing of resonances due to the synchrotron oscillation has been simulated by periodically varying the transverse charge density of the beam.

Although some emittance growth has been observed in the self-consistent treatment, this growth cannot be attributed to the crossing of sextupole resonances. One must find the cause somewhere else including the undesirable dependence on the number of particles tracked. One important result of our study is the clear indication that one must consider the emittance of the beam as a whole instead of changes in the betatron amplitudes of a few selected particles. One is likely to make an unreasonably pessimistic conclusion if a few particles are considered to represent the whole beam.

The treatment of the synchrotron oscillation here is not completely satisfactory. The future study should integrate the longitudinal oscillations in evaluating the self-consistent space charge effect. This would be very time-consuming because of the need to take many more particles in the tracking but it is still feasible with supercomputers such as NEC SX-2 we have used. If there is a clear indication from beam observations in low energy synchrotrons (Fermilab booster, for example) that the emittance growth is observed over longer time periods, it may become necessary to extend the tracking beyond ~ 1000 turns.

Acknowledgements

The author would like to thank Professor Sho Ohnuma for valuable discussions and assistance in preparing the manuscript.

References

- [1] H. Bruck, Particle Accelerators, vol.11, pp.37-44, 1980.
- [2] T. Suzuki, TRIUMF Report, TRI-DN-88-K2, 1988.
- [3] L. K. Chen and M. A. Furman, SSC-164, Nov. 1988.
- [4] G. Parzen, in Proceedings of the 1987 IEEE Particle Accelerator Conference, pp.1182-1184, 1987.
- [5] R. L. Gluckstern, Fermilab Report, TM-1402, 1986.
- [6] L. Schachinger and R. Talman, Particle Accelerators, vol.22, pp.35-56, 1987.
- [7] L. J. Laslett, BNL Report, BNL 7534, 1963.
- [8] I. M. Kapchinskij and V. V. Vladimirkij, in Proceedings of the International Conference on High Energy Accelerators, pp.274-288, 1959.
- [9] J. L. Laclare, G. Leleux, and A. Tkatchenko, Saclay Internal Report, DSS-SOC-RS-74-93/TP-07, 1974.